Journal of Maps

ISSN: 1744-5647 (Online) Journal homepage: www.tandfonline.com/journals/tjom20

# Geomorphology of the lower Mesopotamian plain at Tell Zurghul archaeological site

Giulia Iacobucci, Francesco Troiani, Salvatore Milli & Davide Nadali

**To cite this article:** Giulia Iacobucci, Francesco Troiani, Salvatore Milli & Davide Nadali (2023) Geomorphology of the lower Mesopotamian plain at Tell Zurghul archaeological site, Journal of Maps, 19:1, 2112772, DOI: 10.1080/17445647.2022.2112772

**To link to this article:** https://doi.org/10.1080/17445647.2022.2112772

JOURNAL OF MAPS
2023, VOL. 19, NO. 1, 2112772
https://doi.org/10.1080/17445647.2022.2112772

Taylor & Francis
Taylor & Francis Group

SCIENCE



# Geomorphology of the lower Mesopotamian plain at Tell Zurghul archaeological site

Giulia Iacobucci[a], Francesco Troiani[a], Salvatore Milli[a,b] and Davide Nadali[c]

[a]Dipartimento di Scienze della Terra, SAPIENZA Università di Roma, Roma, Italy; [b]Istituto di Geologia Ambientale e Geoingegneria (IGAG), Consiglio Nazionale delle Ricerche, Montelibretti (Roma), Italy; [c]Dipartimento di Scienze dell'Antichità, SAPIENZA Università di Roma, Roma, Italy

**ABSTRACT**

The landscape of the Lower Mesopotamia Plain (LMP) has been moulded by water-related processes, consequently, its Holocene geomorphic evolution has been strictly connected to the fluvial process and the anthropogenic water management since 8000 BC. About 6000 years ago, during the maximum marine ingression, the modern cities of Nasiriyah and Al-Amara were close to the Persian Gulf shoreline. Successively, the Tigris and Euphrates developed two wide delta systems, that prograded south-eastward developing a complex fluvial network. Remote sensing investigations over the LMP using satellite imagery and topographic analysis revealed the surficial expression of deltaic bodies with a lobate planform and several terminal distributary channels (TDCs), classifiable as tidal-influenced river-dominated deltas. Tell Zurghul archaeological site, belonging to the ancient State of Lagash, expanded in the western part of the recognized TDC during the Mid- and Late Holocene. Indeed, the occurrence of a divergent multi-channel system supplied water for the early civilizations, which improved the water management and prevented floods through a canals network. Therefore, the multi-sensor remote sensing approach over an area of 2850 $km^2$ allowed us to recognize several fluvial landforms, both still active and relict, attributable to the Holocene riverscape of the LMP, as well as anthropogenic features and aeolian deposits. The Main map is a geomorphological map at the scale of 1:120,000 centred on Tell Zurghul, focusing on the geometry, spatial distribution, and state of activity of erosional and constructional landforms.

**ARTICLE HISTORY**
Received 28 January 2022
Revised 20 June 2022
Accepted 3 August 2022

**KEYWORDS**
Waterscape; Lower Mesopotamian Plain; Persian Gulf paleoshoreline; Mid-Holocene maximum marine ingression; Remote Sensing

## 1. Introduction

Geomorphological mapping is an essential tool for analysing and visualising Earth surface features (Otto & Smith, 2013; Reddy, 2018), as well as for reconstructing landscape evolution (Karymbalis et al., 2013; Savelli et al., 2012; Tsanakas et al., 2019). Geomorphological mapping has developed from totally field-based research for a detailed representation of landforms on large-scale maps to more interpretative maps based on remote sensing with limited field checks in inaccessible areas (Knight et al., 2011; Verstappen, 2011). Therefore, since the 1970s, the increasing availability of satellite imageries allowed remote sensing techniques to become increasingly relevant and helpful in geomorphological research (Pavlopoulos et al., 2009). Indeed, in wide and remote areas a small-scale geomorphological mapping can be carried on mosaicking satellite imageries (Bashemina et al., 1979; Postolenko, 1987).

Geomorphological mapping represents a worthwhile research tool, especially when the study area is in intertropical regions under extreme environmental conditions (Bocco et al., 2001). Here, the mapping of each landform and deposit could be quite costly and time expensive. Therefore, remote sensing approaches allow to map landscape features at low and medium cartographic resolution through three mapping approaches: lithological, geomorphological, and pedological (Gürbüz & Gürbüzb, 2022; Napieralski et al., 2013).

The southernmost sector of the Mesopotamian Plain (Iraq), known as the Lower Mesopotamian Plain (LMP), has always sparked the interest of archaeologists, geologists, and geomorphologists, especially because of the long-term interaction between human and environment (Al-Ameri & Briant, 2019; Heyvaert & Walstra, 2016; Morozova, 2005). Indeed, the Middle East has been always considered the cradle of civilization, where the writing, social hierarchization and the taming of nature started, offering an ideal study area for geomorphological analysis focusing on the long-lasting relationship between human and the environment.

CONTACT Giulia Iacobucci giulia.iacobucci@uniroma1.it Dipartimento di Scienze della Terra, SAPIENZA Università di Roma, Piazzale Aldo Moro 5, 00185 Roma, Italy

Supplemental data for this article can be accessed online at https://doi.org/10.1080/17445647.2022.2112772.

During the Holocene, the LMP has been involved into widespread geomorphological and environmental modifications due to post-glacial sea-level rise concomitantly with the sediment supply variations producing an initial transgressive landward migration, followed by a subsequent seaward migration of the Persian Gulf coastline. Moreover, the occurrence of the two longest rivers of the southwest Asia (Cullen & DeMenocal, 2000), the Tigris and Euphrates, has deeply shaped the landscape developing, according to some Authors, wide prograding river delta (Kennett & Kennett, 2006; Lambeck, 1996). Therefore, the question of water within the ancient Mesopotamia has been and still is a central topic in both geomorphological and archaeological research.

This contribution deals with the analysis of the function and the role of water within a complex environmental system that encompasses natural and anthropic features all over the ancient State of Lagash between the latitude of 31°10′00″ N and 31°35′00″ N (Dhi Qar and Misan governorates), adopting remote sensing techniques for the geomorphological mapping of both active and inactive fluvial landforms, as well as their reworking mainly due to human activities and aeolian processes. Indeed, the reconstruction of the Mesopotamian landscape provides a challenging research topic, especially if we consider the reconstruction of the Persian Gulf shoreline during the Mid-Holocene maximum marine ingression. In this regard, multi-sensor remote sensing techniques based on satellite imagery and topographic analysis from DEMs are a particularly useful approach for investigating remote and wide areas, especially when the landscape is rather barren (Iacobucci et al., 2020). In this study, fluvial, aeolian, and anthropic features were detected and mapped at the scale of 1:120,000, according to a morphographic, morphogenetic, and morphodynamic classification approach. The inactive fluvial landforms were also compared to the topographic and geomorphological features that can reasonably express the effects of the maximum marine ingression during the Holocene to highlight the waterscape dynamic changes under the effects of the sea-level variations.

When dealing with the morphoevolution of the LMP during the Holocene, at least two types of processes connected with water must be considered: natural processes related to rivers and sea, and artificial processes related to hydraulic works for the running water management like the construction of canals. Indeed, the modern drainage planform pattern is rather different from the previous one, as well-demonstrated by recent studies where the combination of geological, geomorphological, historical, and archaeological approaches (Hritz & Wilkinson, 2006; Jotheri et al., 2016; Jotheri et al., 2018) highlighted that fluvial processes, human activities (De Klerk & Joosten, 2021; Forti et al., 2022; Heyvaert et al., 2012; Jotheri et al., 2018; Wilkinson et al., 2015), and neotectonics (Fouad, 2010; Sissakian et al., 2014; Sissakian et al., 2020) played a relevant role in the Holocene morphoevolution of the area.

## 2. Study area

The LMP coincides with the lowermost sector of the Tigris and Euphrates rivers alluvial plain. The Tigris drains the eastern part of the plain, while the Euphrates flows through the western zone. About 170 km inland from the present-day shoreline of the Persian Gulf, the two rivers join to form the Shatt-al-Arab river; this latter flows through the wide marshland area of Qurna, forming in the proximity of the coast an estuarine mouth (Al-Ameri & Briant, 2019; Jotheri et al., 2018).

The LMP, as well as the northernmost sector known as Upper Mesopotamian Plain (UMP), constitutes a subsiding foreland basin developed during the late Cenozoic and formed as the consequence of the subduction of the Arabian Plate under the Eurasian Plate. Arabo-Eurasian convergence started during the Late Jurassic. From the Late Oligocene to the Early Miocene, the continental collision caused the lithospheric flexure of the Arabian Plate and the beginning of the deposition in the Mesopotamia foreland basin. During the Miocene and Pleistocene, the ongoing Arabia-Eurasia convergence involved deformation and deposition giving rise to the formation of the Zagros fold-and-thrust belt (Alavi, 2007; Saura et al., 2015; Sissakian et al., 2013; Sissakian et al., 2020).

The Mesopotamian lowlands are composed of 15–20 m thick Holocene terrigenous sediments made up of sand, silt, and mud, which are attributed to the fluvio-lacustrine, estuarine, and deltaic depositional environments (Yacoub, 2011). Precisely, the Holocene sediments can be sub-divided into three stratigraphic units from bottom to top (Aqrawi, 2001): Unit 1, is constituted by a lower fluvial sandy unit with gypcretes and floodplain deposits; Unit 2 is made of estuarine brackish/marine deposits; Unit 3 is composed by fluvio-lacustrine deposits. Units 1 and 2 are transgressive having been deposited during the Holocene sea-level rise and they are Early-Mid-Holocene in age. Unit 3, developed during the Holocene highstand phase and shows a typical progradational trend (Aqrawi, 1995a, 1995b, 2001; Yacoub, 2011); it is late Middle and Upper Holocene in age.

Specifically, during the Early Holocene, a wide fluvial system prevails in the area, being part of the Persian Gulf in subaerial condition with the shoreline located southward than the modern one (Lambeck, 1996). During the Mid-Holocene (about 6000 yr BP), the rapid sea-level rise promoted the landward migration of the shoreline reaching the maximum

inland position in correspondence with the alignment between the cities of Nasiriyah and Amarah (Aqrawi, 2001; Forti et al., 2022; Kennett & Kennett, 2006; Milli & Forti, 2019; Pournelle, 2003). Between the Mid- and Late Holocene, a shift from humid to arid climatic conditions occurred (Engel & Brückner, 2021; Nehme et al., 2018 and references therein) that produced a significant decrease in the Tigris and Euphrates deltaic progradation. The complex of fluvial channels was gradually abandoned, and the current fluvial pattern began to emerge (Aqrawi, 1995a, 2001; Morozova, 2005; Sanlaville, 1989, 2003). Freshwater conditions continued for about 3000 years (Aqrawi & Evans, 1994; Altaweel, 2019); the Gulf reached its current configuration around AD 1000 as a result of the Shatt Al-Arab delta's progradation south of Basrah (Al-Hamad et al., 2017; Aqrawi, 2001; Bogemans et al., 2017). Although the exact position of the shoreline at 6000 yr BP is still discussed, in agreement with Jotheri et al. (2018), the marine transgression never reached the Uruk area (about 300 km far from the present shoreline), confirming that the inactive fluvial channels recognized in the Nasiriyah and Al-Amara area are likely linked to the Euphrates and Tigris paleo-deltas.

The present study focuses on the area of about 2850 km$^2$ comprises between the latitude of 31°10′00″ N and 31°35′00″ N (Figure 1). The archaeological site of Tell Zurghul is located 40 km ca. north-eastward from the city of Nasiriyah, with an area of 70 ha characterized by two mounds. The highest Mound A and the lower Mound B, with an altitude range from 8 up to 15 m a.s.l, are the key sectors where the evidence of the early formation of the settlement is preserved (Nadali, 2021; Nadali & Polcaro, 2020).

The ancient Sumerian State of Lagash included the cities of Girsu, Lagash, Tell Zurghul, and the likely Guabba, where several irrigation systems dating to the Early Dynastic Period (Early III millennium BCE) were identified in the area (Nadali, 2021). Indeed, the shape and the extension of the sites are strongly influenced by the surrounding ecosystem, where water played a prominent role and needed regulation through the care of canals and the management of floods (Nadali & Polcaro, 2020; Nadali, 2021; Steinkeller, 2001). In this manner, the occurrence of water in the ancient LMP favored the birth and the economic growth, as well as the social and political development of several cities (Algaze, 2001; Nadali, 2021; Wilkinson et al., 2015).

The alluvial and deltaic landscape of the LMP covers much of the Mesopotamian depression and includes both active and inactive, low-gradient alluvial plains, anastomosing and meandering rivers, levees above the surrounding floodplains, crevasse splays and canals. Moreover, aeolian landforms such as deflation surfaces and blow-outs characterize the area (Engel & Brückner, 2021; Jotheri et al., 2018; Sissakian et al., 2020). In the southern part of the LMP large-scale marshlands (called typically *ahwar*) are frequent at the confluence of Euphrates and Tigris watercourses, downstream through the Shatt al-Arab River floodplain and estuarine area. The central area of the LMP is occupied by the Holocene fluvial deposits of both the Tigris and Euphrates, as well as by a wide range of continental and paralic environments developed under the influence of Holocene climate oscillations and sea-level fluctuations (Aqrawi, 2001; Milli & Forti, 2019; Yacoub, 2011).

## 3. Materials and methods

A remote sensing approach were adopted using products derived from different Earth observation missions in combination with site-specific field geomorphological surveys performed during several archaeological campaigns. The remote sensing methodological approach considers: (i) a preliminary visual inspection of the study area through optical satellite imagery; (ii) the topographic analysis considering the optical digital topographic dataset derived from AW3D30 Digital Surface Models; (iii) the computation of multispectral indices like *Normalized Difference Vegetation Index* and *Clay Ratio* (NDVI and CR, respectively). The methodological approach agrees with the one proposed by Iacobucci et al. (2020) who demonstrated as the use of optical and multispectral satellite imagery, in combination with the digital topographic data, is a valid tool for a remote investigation of lowland and barren areas like the LMP (Brink & Eva, 2009; El-Gammal et al., 2014).

Since the LMP has been deeply modified by human activities over millennia, the improved geomorphological legend proposed by Vergari et al. (2020) has been adopted for classifying and representing landforms due to natural processes that experienced anthropogenic modifications. Therefore, the state of activity defined as 'modified' has been added to the traditional 'active' and 'inactive' ones in the geomorphological map legend and has been used to refine the state of activity of the fluvial and crevasse channels.

### 3.1. Preliminary inspection

Freely available optical satellite imagery, such as the ESRI® TerraColor of the ArcGIS 10.8.1 software package and the Google® Earth virtual globe datasets, were employed during the preliminary recognition of active and inactive fluvial landforms which surround the archaeological site of Tell Zurghul.

The Google® Earth time-lapse spans the period 1984–2016, with a maximum geometric resolution of 2.5 m obtained by SPOT imagery, allowing a multitemporal observation of the area. Furthermore, TerraColor NextGen imagery from Earthstar Geographics

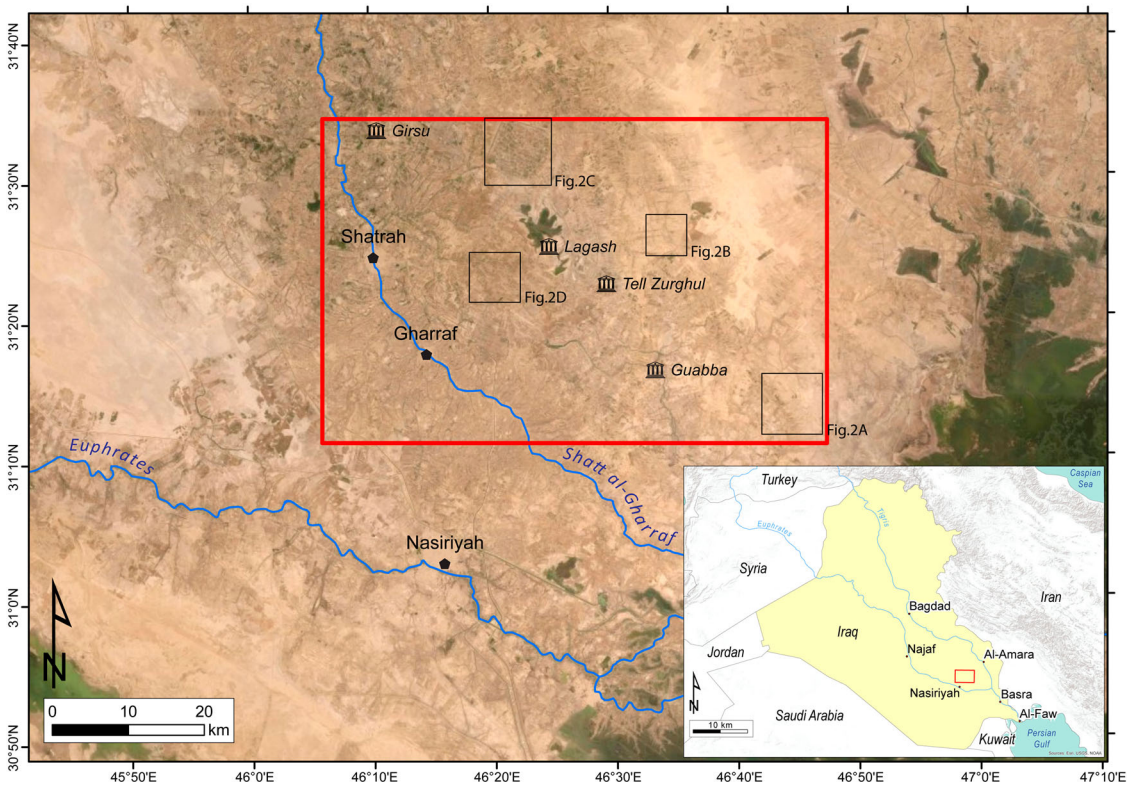


**Figure 1.** Satellite imagery (ESRI TerraColor NextGen) of the study area (red rectangle) and the location of satellite imageries in Figure 2 (black squares).

added more distinctive and natural colour, with a geometrical resolution of 15 and 2.5 m for the study area (Waterman, 2020).

Four key optical features were considered for recognizing and mapping active and inactive channelized landforms, such as colour, pattern, shape, and situation (Jotheri, 2018; Jotheri & Allen, 2020). The colour is a key feature especially for discerning the state of activity of fluvial landforms, since the greenish pixels prevail in the active features, while the inactive fluvial channels are yellowish-brownish. The pattern and shape are also essential for discerning fluvial channels from the irrigation canals: the first ones have a high sinuosity, both meandering and anastomosing pattern with several divergent branches, frequently associated to scroll bars along the inner zone of the channel belt, while the irrigation canals have a single more straightened canal with a herringbone or trellis spatial distribution (Figure 2). Finally, the occurrence of already recognized avulsion processes (Iacobucci et al., 2020) leads to considering the situation, since the presence of an inactive crevasse splay can be undoubtedly linked to a parent channel. Moreover, some anthropic features are considered in the situation like the occurrence of small villages and the size of irrigated croplands.

### 3.2. Topographic analysis

Considering the vertical accuracy of AW3D30 DSM of 5 m as reported by Uuema et al. (2020), we have selected a 1–5 m pixel altimetry re-classification scheme, starting from the sea level up to the maximum elevation. In this manner, the low topographic relief of the fluvial and anthropic features is better visualized, especially for the 1-m interval, where the higher elevation with respect to the surrounding floodplain relating to archaeological mounds, channel levees, crevasse splays, and canals are more accentuated (see also Iacobucci, 2021; Iacobucci et al., 2020; Jotheri et al., 2018; Jotheri & Allen, 2020).

Using the *Reclassify Tool* available in ArcGIS 10.8.1, the AW3D30 elevation data has been reclassified considering two new classes: values below 6 m and values above 6 m. In this manner, a presumable reconstruction of the shoreline morphology during the maximum marine ingression phase has been possible (Iacobucci, 2021). Lambeck (1996) proposed a sea-level rise of 2–3 m around Al-Faw, but the adopted value of 6 m complies with the on-surface artefacts that affected the AW3D30 DSM, despite the study area being quite barren.

The section AA' has been considered to distinguish the sub-areas of the waterscape (i.e. inactive and active fluvial channels, marshlands, floodplains, irrigation canals, and archaeological mounds) by their elevation above the floodplain and the photointerpretation of the optical dataset. The section has been smoothed by applying a moving average filter of 30 m for removing the 'on-surface noise' that affected the AW3D30 DSM.

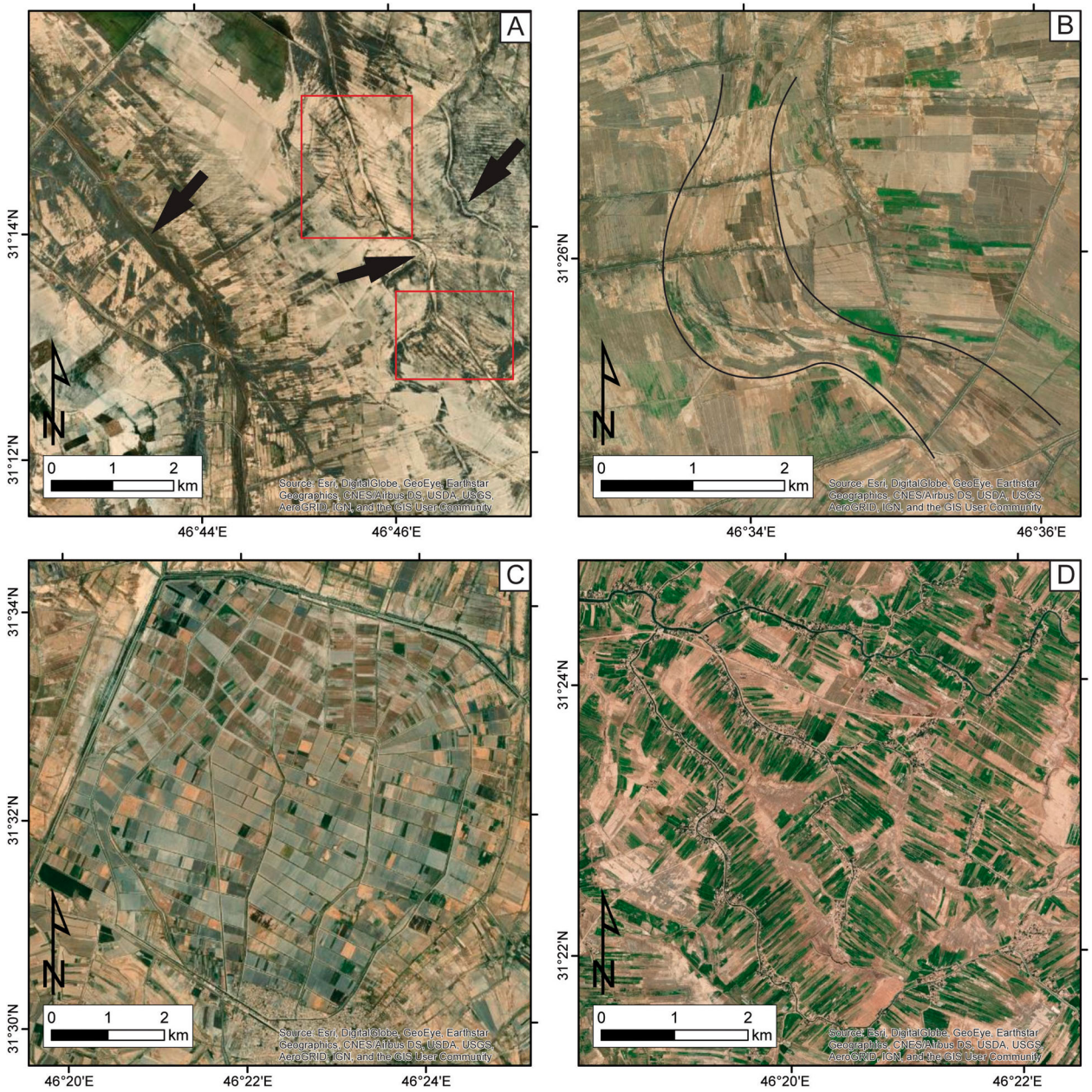


**Figure 2.** Satellite imageries (ESRI TerraColor NextGen) of inactive fluvial channels (A, B), active canals (C), and the active fluvial channels with the perpendicular herringbone pattern of the crops (D). In Figure 2A, the black arrows point out the yellowish-brownish features of the inactive fluvial channels, while the red rectangles highlight the herringbone pattern of inactive canals. In Figure 2B, the black lines point out the ridge-and-swale texture of the scroll bars.

### 3.3. Multispectral indices: NDVI and CR

The Landsat series is one of the first Earth observation missions launched in 1972 with a moderate resolution (https://earth.esa.int/eogateway/missions/landsat). Thus, it is perfect for a remote investigation of a barren landscape like the LMP, especially for defining the state of activity of fluvial landforms. Indeed, multispectral imagery can detect the difference in reflectance properties of fluvial deposits when their chemical-mineralogical composition and micro-relief change (D'Arcy et al., 2018; Iacobucci et al., 2020; Kahle et al., 1984).

Through the USGS Earth Explorer interface, we have selected 12 imageries collected during the wettest (October–December) and the driest (July–August) periods of 2017, considering the lowest land cloud cover. In this manner, different conditions of reflectance can enhance variation in soil moisture, vegetation cover, and amount of suspended materials along the watercourses.

The spectral indices NDVI and CR have been considered for defining the state of activity of fluvial channels, crevasse splays, and floodplains since the highest values of NDVI help to identify the wettest sectors where watercourses are still active. Instead, the CR allows us to identify clayey-silty distal deposits of crevasse splays and floodplains. Considering the sedimentological composition of the LMP is made of

sandy, silty, and clayey deposits, the lowest value of CR should correspond to the sandiest ones.

## 4. Results and discussion

### 4.1. Landforms due to fluvial process

The study area can be distinguished into two sub-areas: the active floodplain of the Shatt al-Gharraf River in the western part (1600 km$^2$), and the inactive floodplain of the Dujaila channel eastward (1200 km$^2$). Both the Shatt al-Gharraf and Dujaila floodplains belong to the Tigris River system, which influences their water storage and flood dynamic. The state of activity of these two sectors is clearly shown by the highest values of NDVI and CR in the western floodplain (Figure 3). Indeed, the latter is mainly influenced by human activity, essentially farming, where the dendritic and trellis drainage pattern of the Shatt al-Gharraf's distributaries guarantees the irrigation of the proximal surrounding croplands, while the farther ones are irrigated by canals.

The crop size is a useful parameter for distinguishing channels and canals since it seems to be linked to which kind of watercourses irrigate it. For example, crops surrounding channel banks are less than 1 km elongated from the channel itself and frequently interrupted by small villages. On the other hand, canals support the growth of wider crops (40–50 ha) out of urbanized areas, also reaching the ones in the inactive Dujaila floodplain, northward to Tell Zurghul.

The trellis pattern of the Shatt al-Gharraf distributaries might suggest the strong influence of human management over the drainage pattern, allowing the mapping of the modified branches and reaches in the Shatt al-Gharraf floodplain. On the other hand, the inactive floodplain of the Dujaila channel still preserves several inactive watercourses belonging to an anastomosing system. Indeed, the high sinuosity of the fluvial channels, several scrollbars, convex-up intra floodbasins, and inactive crevasse splays of assorted sizes suggest higher lateral mobility of this system than the western active one. However, inactive crevasse splays are still recognizable along the Shatt Al-Gharraf, where most of the crevasse channels have been modified and used as irrigation canals, especially in the southern sector. Here, partially preserved inactive crevasse channels with high sinuosity allowed the mapping of the crevasse splays themself.

Both the active and inactive fluvial channels are characterized by several metres of elevation above the floodplain, namely 2–3 m, with extensive levees of 1–2 km, especially where no anthropogenic modifications occurred. Indeed, the modified fluvial channels of the western sector are considerably narrower and lower (i.e. 1 m ca.), essentially due to the construction of the artificial levees and the occurrence of crops along their banks. Similarly, the modified crevasse channels are more detectable than inactive ones thanks to their higher elevation, despite the inactive crevasse channels being well recognizable in the optical and multispectral data (Figure 4). Indeed, the reworking of crevasse channel deposits prevents their recognition through the multispectral supervised classification or visual inspection (e.g. Iacobucci et al., 2020), but their topography can be potentially preserved favouring their mapping through the topographic analysis.

The marshland of Hawr al Ghamukah surrounding the archaeological site of Lagash is partially fed by the Shatt al-Gharraf branches and its maximum size of about 38 km$^2$ is reached during the wettest period. The banks are characterized by high values of NDVI suggesting the occurrence of herbaceous plants, while the highest values of CR provide the prevalence of clayey deposits. Its distance from the modern shoreline might suggest it is an inland freshwater marsh, although the reconstruction of the maximum marine ingression shoreline could suggest that it was a coastal marsh during the Mid-Holocene. Several smaller marshes are also recognizable along the Shatt al-Gharraf, principally used for farming.

### 4.2. Anthropogenic landforms

The anthropogenic landforms are essentially represented by irrigation canals, archaeological mounds and urban areas. These last are not so extended, taking up only 1.5% of the study area and corresponding to the cities of Al Neser, Shatrah, and Gharraf.

The irrigation canals are characterized by parallel and herringbone patterns, while their straightness avoids frequent clogging and siltation. These differences allow us to distinguish the canals from the active fluvial channels during the visual inspection; anyway, the topographic analysis highlights another difference between active fluvial channels and canals, where these last are rather low with an elevation of 1 m or less above the surrounding floodplain. However, most of the canals in the north-eastern sector to Tell Zurghul have the same direction as the paleochannels, partially deleting their traces (Figure 5).

Despite the lack of dated field data, we can infer most of the mapped canals are essentially modern infrastructures mainly W-E oriented, especially those in the active floodplain of the Shatt al-Gharraf and northward of Lagash. Through the multitemporal acquisition of Google® Earth, we can appreciate how the central sector of the study area progressively shifted toward more arid conditions, with the decreasing of Hawr al Ghamukah marhland from 70 km$^2$ in December 1988–35 km$^2$ nowadays. Therefore, we suppose central canals of the Dujaila floodplain could be potentially archaeological elements re-used over

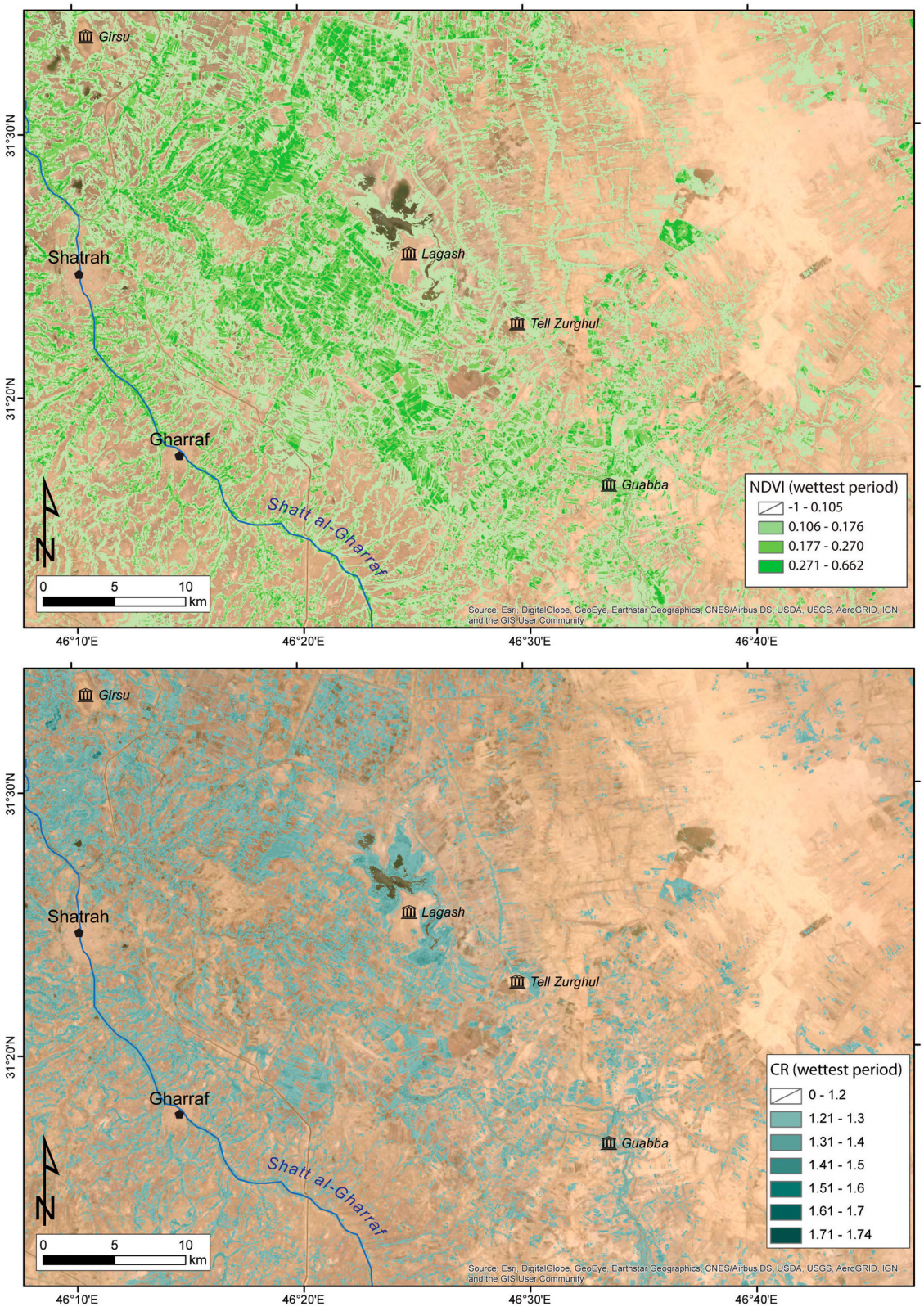


**Figure 3.** The multispectral indices NDVI and CR; the highest values of both indices are in the westernmost sector over the active Shatt al-Gharraf floodplain.

time, since their position is frequently close to the traces of abandoned channels, with N-S orientation. The latter progressively dried out during the Upper Holocene, forcing the locals to dig new irrigation canals and tackle siltation in the priors through their rectification.

Girsu, Lagash, and Tell Zurghul are historically recognized as part of the State of Lagash (about 6000 yr BP), while the location of Guabba is only supposed since its topographic expression, as well as the archaeological evidence, are rather scarce. Their typical elliptical shape and their elevation of about 3–

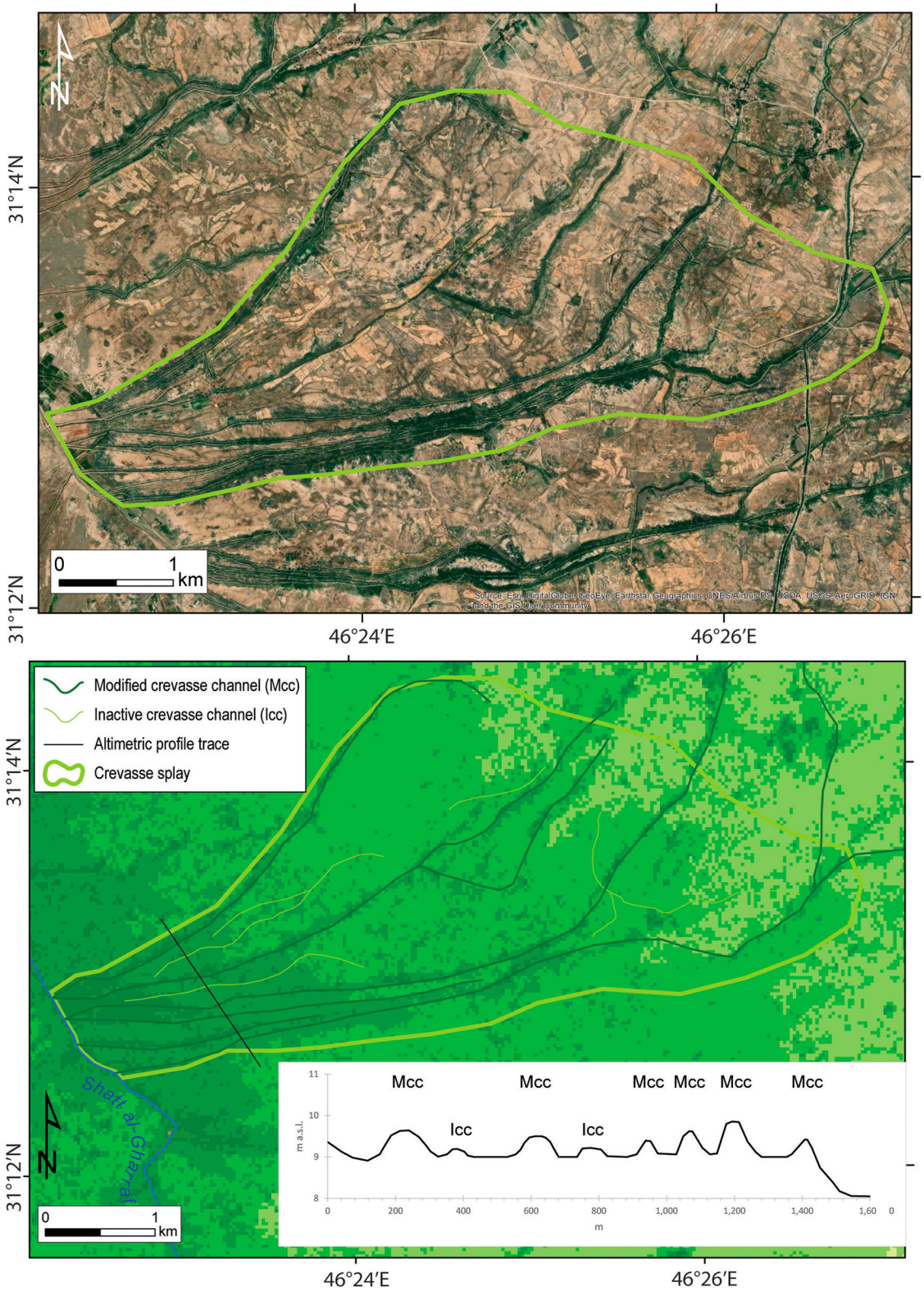


**Figure 4.** Satellite view (A) and AW3D30 DSM (B) where the altimetric profile has been constructed along an inactive crevasse splays on the right bank of the Shatt al-Gharraf. The modified crevasse channels (MCC) are higher than the inactive crevasse channels (ICC).

6 m above the surrounding floodplain are the main characteristics of their detection during the visual inspection and the topographic analysis. The archaeological mounds are characterized by a flat summit surface and steeper slopes than the channel levees.

Tell Zurghul (Figure 6) and the hypothetical Guabba are the closest archaeological sites to the westernmost TDC, while Girsu is closer to the Shatt al-Gharraf River. Both Tell Zurghul and Guabba are only 2.5 km distant from the limit of the TDC, in

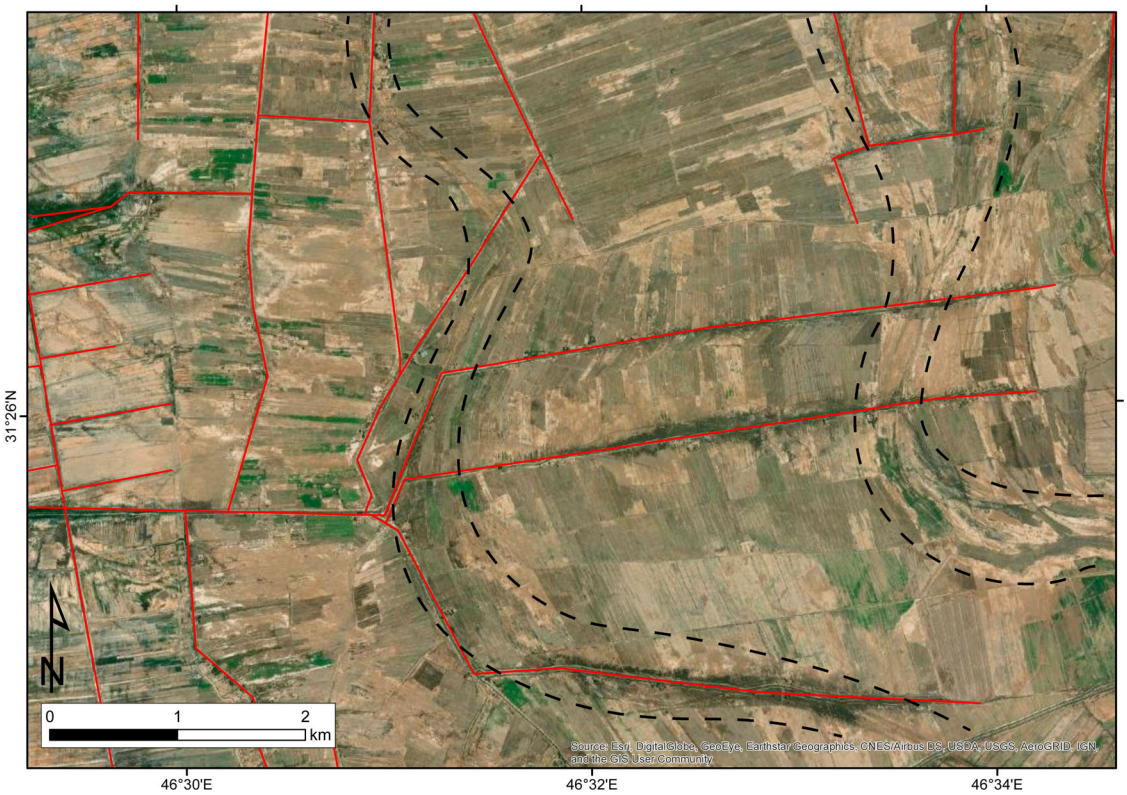


**Figure 5.** The irrigation canals mapped with red lines partially overlap the inactive fluvial channels traced by black dotted lines.

intra floodbasins delimited by the abandoned distributary channels of the anastomosing system.

Girsu, Lagash, Tell Zurghul, and partially Guabba are elevated mounds in sunken areas. This allows us to suppose that the occurrence of floods guaranteed the irrigation of surrounding crops, preventing the flooding of buildings.

### 4.3. Landforms due to aeolian processes

The easternmost sector of the study area is barren and lacks clayey deposits, as confirmed by the lowest values of NDVI and CR in Figure 3. Similarly, the archaeological sites appear with the same peculiarities. Anyway, the origin of these sandiest deposits might be quite different: archaeological sites like Girsu and Tell Zurghul present a typical radial drainage pattern (e.g. Jotheri, 2016) due to gully erosion and transport of the finer deposits. On the other hand, the sandiest deposits of eastern sector could be linked to both aeolian processes and high human pressure. The easternmost sector preserves wide deflation surfaces of about 100–700 km$^2$, where the semi-arid condition and the lack of vegetation support the development of loose terrain susceptible to chemical weathering and deflation (Laity & Bridges, 2013). Indeed, the study area is frequently hit by severe dust storms in late spring and summer, mainly due to local winds like *Shamal* which blows from northwest (Figure 7). Google® Earth imageries detect several abandoned crops and canals, especially in the north-eastern sector, suggesting us the occurrence of these bare areas is also the consequence of overgrazing and high human pressure, as also demonstrated by Wilkinson et al. (2015).

### 4.4. Morphological reconstruction of the mid-Holocene inland delta

The raster reclassification starting from the adopted DEM, in the ArcGIS 10.8.1 software, allows for a rough, preliminary digital topographic simulation of the position of the Persian Gulf shoreline during the Mid-Holocene maximum marine ingression, pointing out a more detailed morphology of the shoreline in the context of the deltaic evolution of the area. In the latter, the easternmost sector preserves several inactive branches of the Dujaila multi-channel system, where the simulation of the maximum marine ingression closes off four distal channelized features known as terminal distributary channels (TDCs). These last are the channels of a prograding delta system, that are well developed in the study area thanks to the physiographic characteristics of the Persian Gulf: a large cul-de-sac open south-eastward, where the strong interaction between fluvial and tidal processes was likely amplified by tides (see Ashworth et al., 2015; Bhattacharya, 2006; Forti et al., 2022; Giosan & Bhattacharya, 2005; Hoitink et al., 2017; Olariu & Bhattacharya, 2006 for more discussion on delta processes). Recognized landforms like distributary channels, intra floodbasins, levees above the floodplain,

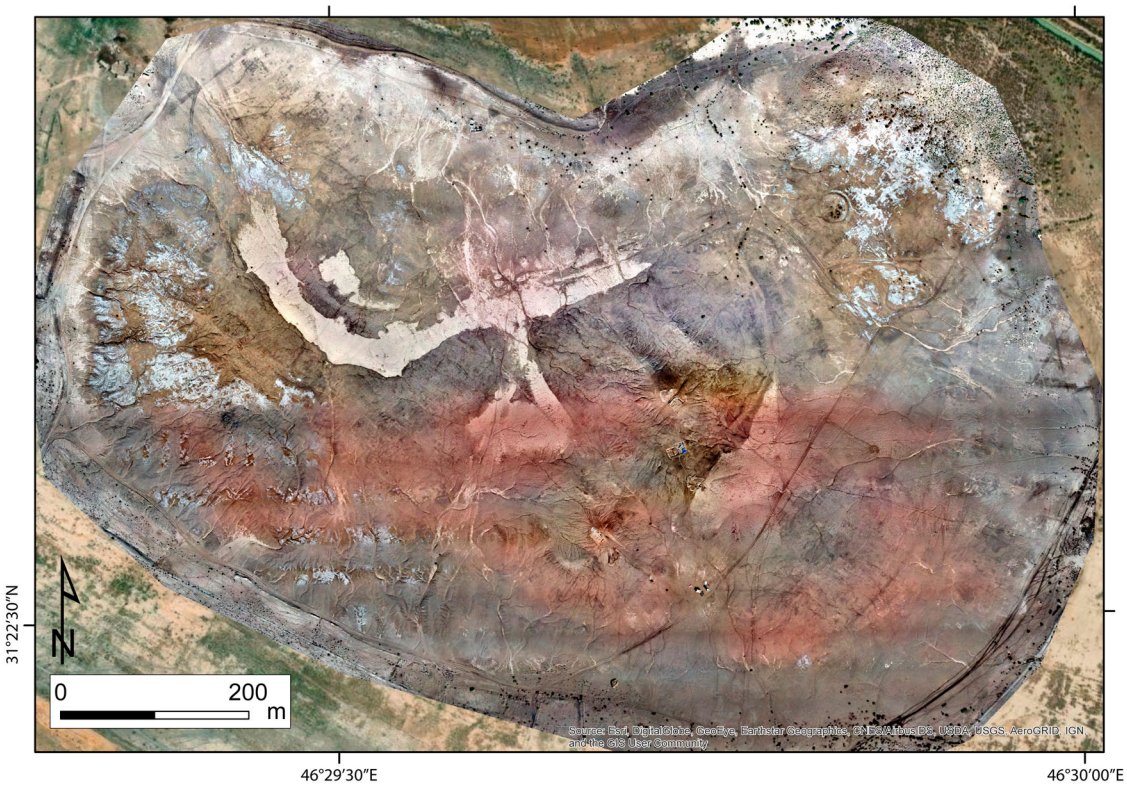


**Figure 6.** The UAV orthophoto of Tell Zurghul archaeological site acquired on 2017 (MAIN© Missione Archeologica Italiana a Nigin).

and crevasse splays infer the occurrence of a river-dominated, tidal-influenced delta (Forti et al., 2022; Iacobucci, 2021).

The TDCs are still recognizable thanks to their elevation above the modern floodplain, in addition to their high-sinuosity and a meandering pattern. Despite the inactive branches of the Dujaila being recognized as inactive fluvial channels, their morpho-dynamic during the maximum marine ingression should be influenced by the proximity of the sea. Only four main branches, characterized by a single meandering channel, would seem to prograde southward and eastward in the Persian Gulf for several tens of kilometres. For example, TDC1 is the longest one, with a length of 55 km and a width of 1–3 km. Moving eastward, TDC2 is considerably shorter and the widest one (33 and 4 km, respectively), where the visual inspection identified almost two main channels. TDC3 is the narrowest one (0.5–2 km) and is most likely linked to the easternmost TDC4. This last is rather long and narrow (40 km and 1,5 km, respectively), but the occurrence of a

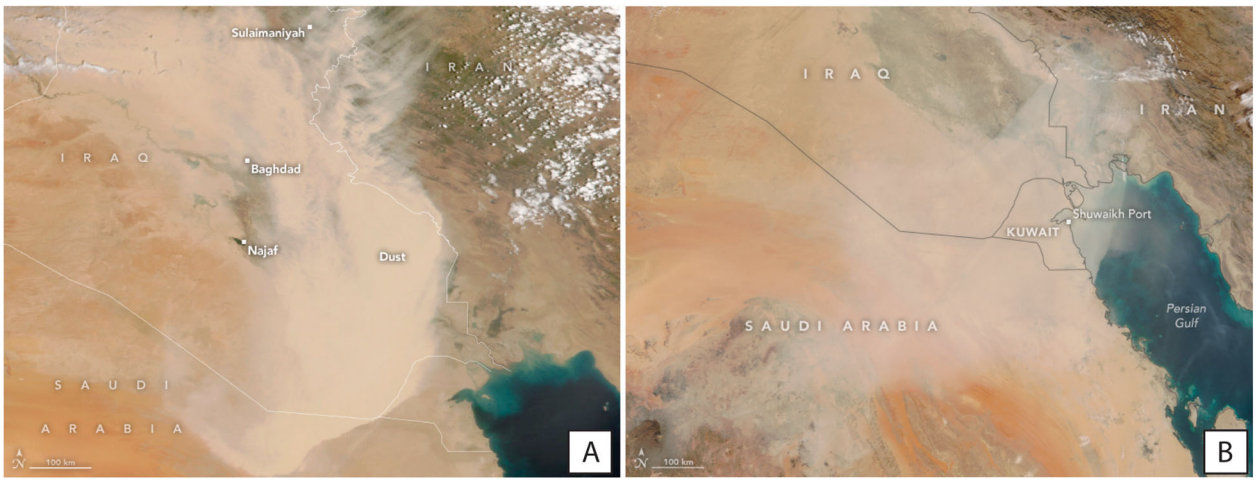


**Figure 7.** Natural-color images acquired by MODIS instruments carried by Terra and Aqua Satellites. Severe dust storms over Iraqi territory dated on 16 May 2022 (A) and 31 October 2017 (B). Images available online at NASA Earth Observatory (n.a.) website (https://earthobservatory.nasa.gov/images)

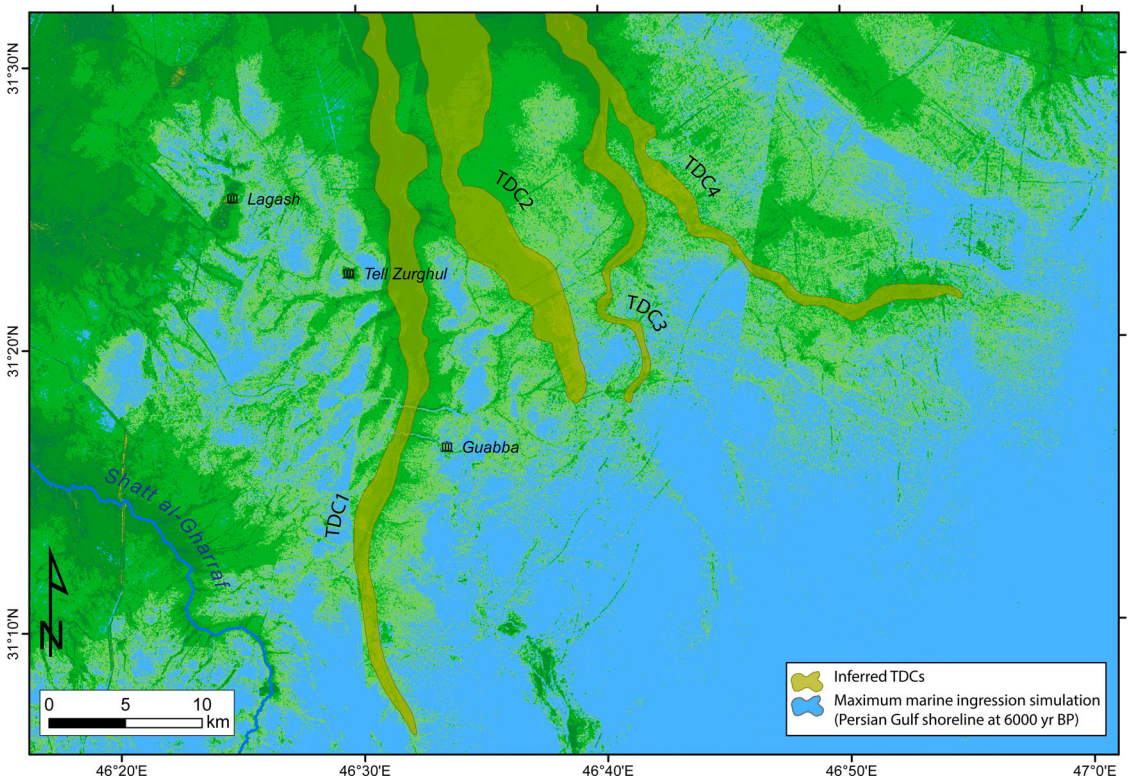


**Figure 8.** The AW3D30 reclassification where the four main TDCs of the study area are recognized and mapped.

DEM error prevents its reliable reconstruction (Figure 8).

The occurrence of several scrollbars along both the banks of each TDC suggests the high mobility of these landforms, favouring their width increasing, while the occurrence of the crevasse splays should be linked to the following anastomosing pattern that occurred after the southward shifting of the Persian Gulf shoreline. Indeed, the low gradient between the TDC and the surrounding delta plain favoured the development of a poorly incised channel, without well-developed levees. Thus, flood events involved lateral mobility rather than levee breaks.

Due to the progradation of the delta system and the southwards shift of the Persian Gulf shoreline, the TDCs modified their morphodynamics becoming the distributary branches of the multi-channelized system of the Dujaila and scarcely preserving the TDC features.

## 5. Conclusions

Active and inactive landforms, mainly fluvial, are recognized in the study area, which can be better defined as a waterscape. Indeed, the water is the main geomorphic agent, acting as fluvial processes along two main fluvial features (i.e. the active Shatt al-Gharraf and the inactive anastomosed Dujaila). However, the historically human presence in the area deeply modified the LMP waterscape, essentially through the construction of irrigation canals that are frequently located in the same traces of the inactive fluvial channels, making difficult their recognition. Moreover, the modern semi-arid climatic conditions favour aeolian processes that rework either inactive landforms like channels or archaeological mounds, especially where loose soils are developed by chemical weathering, gully erosion, and overgrazing. Due to the increasing frequency and intensity of sand and dust storms during the last decades in Iraq, especially in the LMP (Middleton, 1986; Moridnejad et al., 2015; Sissakian et al., 2013), the easternmost sector preserves wide sandy deflation surfaces.

Despite poorly geochronological constraints, the geomorphological analysis of the area, which combines elevation data and multispectral imagery, allows recognizing and mapping of active, inactive, and modified features at the small cartographic scale, as well as allowed to estimate the surficial geometry and the location of the Persian Gulf ancient shoreline during the maximum marine ingression at 6000 yr BP. This allows us to better specify the morphodynamic of the distal channelized features, classifying them as TDCs.

The geomorphological mapping at small scale adopting a remote sensing approach is feasible in semi-arid environments, especially when the field investigation of a wide area could be compromised by social and political conflicts, international lockdowns, or logistic difficulties. Nonetheless, it must be emphasized that field-based data are essential in geomorphological mapping and recommended to

confirm or reject the remote sensing interpretations, especially for the constructional landforms, adding ground-truth information to the mapped landscape features at a more detailed, local cartographic scale.

## Software

The map and the layout were produced using ESRI® ArcGIS 10.8.1 and Adobe Illustrator CC 2019. The multispectral analysis of the Landsat 8 imagery has been conducted on ENVI® 5.3.

The map was embedded into the A1 size, adding as separate inset (i) the location map of the Tigris-Euphrates River delta during the maximum marine ingression of the Persian Gulf; and (ii) the altimetric profile along NW-SE trending track along with the distribution of the crossed landforms are reported.

## Disclosure statement

No potential conflict of interest was reported by the author(s).

## Funding

This work was supported by the grant from the Italian Ministry of Instruction, University and Research (MIUR) to Prof. Davide Nadali (PRIN Project, 2017NMK5FE "Fluid Crescent. Water and Life in the Societies of the Ancient Near East").

## Data availability statement

The data that support the findings of this study are available from the corresponding author, Iacobucci G., upon reasonable request.

## References

Al-Ameri, I. D. S., & Briant, R. M. (2019). A late Holocene molluscan-based palaeoenvironmental reconstruction from southern Mesopotamia: Implications for the palaeogeographic evolution of the Arabo-Persian gulf. *Journal of African Earth Sciences*, *152*, 1–9. https://doi.org/10.1016/j.jafrearsci.2018.12.012

Alavi, M. (2007). Structures of the Zagros fold-thrust belt in Iran. *American Journal of Science*, *307*(9), 1064–1095. https://doi.org/10.2475/09.2007.02

Algaze, G. (2001). Initial social complexity in southwestern Asia. The Mesopotamian advantage. *Current Anthropology*, *42*(2), 199–233. https://doi.org/10.1086/320005

Al-Hamad, S. S., Albadran, B. N., & Pournelle, J. R. (2017). Geological history of Shatt Al-Arab River, South of Iraq. *International Journal of Science and Research*, *6*(1), 2029–2039. https://doi.org/10.21275/ART20164492

Altaweel, M. (2019). Southern Mesopotamia: Water and the rise of urbanism. *Wires Water*, *6*(4), e1362. https://doi.org/10.1002/wat2.1362

Aqrawi, A. A. M. (1995a). Correction sedimentation rates for mechanical compaction: The Tigris and Euphrates Delta, lower Mesopotamia. *Marine and Petroleum Geology*, *12*(4), 409–416. https://doi.org/10.1016/0264-8172(95)96903-4

Aqrawi, A. A. M. (1995b). Brackish-water and evaporitic Ca-Mg carbonates in the Holocene lacustrine/deltaic deposits of southern Mesopotamia. *Journal of the Geological Society*, *152*(2), 259–268. https://doi.org/10.1144/gsjgs.152.2.0259

Aqrawi, A. A. M. (2001). Stratigraphic signatures of climatic change during the Holocene evolution of the Tigris-Euphrates Delta, lower Mesopotamia. *Global and Planetary Change*, *28*(1-4), 267–283. https://doi.org/10.1016/S0921-8181(00)00078-3

Aqrawi, A. A. M., & Evans, G. (1994). Sedimentation in the lakes and marshes (Ahwar) of the Tigris-Euphrates Delta, southern Mesopotamia. *Sedimentology*, *41*(4), 755–776. https://doi.org/10.1111/j.1365-3091.1994.tb01422.x

Ashworth, P. J., Best, J. L., & Parsons, D. R. (2015). Fluvial-tidal sedimentology. In P. J. Ashworth, J. L. Best, & D. R. Parsons (Eds.), *Developments in sedimentology* (Vol. 68, pp. 634). Elsevier.

Bashemina, N. V., Leont, O. K., & Tal Skaya, N. N. (1979). The world geomorphological map in the scale 1:15,000,000. *Geologiya i Geofizika*, *3*(231), 134–137. https://eurekamag.com/research/020/474/020474785.php

Bhattacharya, J. P. (2006). Deltas. In H. W. Posamentier, & R. G. Walker (Eds.), *Facies models revisited* (pp. 237–292). Special Publication 84. SEPM (Society for Sedimentary Geology). https://doi.org/10.2110/pec.06.84.0237

Bocco, G., Mendoza, M., & Velàzquez, A. (2001). Remote sensing and GIS-based regional geomorphological mapping—A tool for land use planning in developing countries. *Geomorphology*, *39*(3-4), 211–219. https://doi.org/10.1016/S0169-555X(01)00027-7

Bogemans, F., Boudin, M., Janssens, R., & Baeteman, C. (2017). New data on the sedimentary processes and timing of the initial inundation of lower Khuzestan (SW Iran) by the Persian Gulf. *The Holocene*, *27*(4), 613–620. https://doi.org/10.1177/0959683616670224

Brink, A. B., & Eva, H. D. (2009). Monitoring 25 years of land cover change dynamics in Africa: A sample based remote sensing approach. *Applied Geography*, *29*(4), 501–512. https://doi.org/10.1016/j.apgeog.2008.10.004

Cullen, H. M., & DeMenocal, P. B. (2000). North Atlantic influence on Tigris–Euphrates streamflow. *International Journal of Climatology*, *20*(8), 853–863. https://doi.org/10.1002/1097-0088(20000630)20:8<853::AID-JOC497>3.0.CO;2-M

D'Arcy, M., Mason, P. J., Roda-Boluda, D. C., Whittaker, A. C., Lewis, J. M. T., & Najorka, J. (2018). Alluvial fan surface ages recorded by Landsat-8 imagery in Owens Valley, California. *Remote Sensing of Environment*, *216*, 401–414. https://doi.org/10.1016/j.rse.2018.07.013

De Klerk, P., & Joosten, H. (2021). The fluvial landscape of lower Mesopotamia: An overview of geomorphology and human impact. IMCG Bulletin 2021-3: May–June 2021, pp. 6–20.

El-Gammal, M., Ali, R. R., & Eissa, R. (2014). Land use assessment of barren areas in Damietta Governorate, Egypt using remote sensing. *Egyptian Journal of Basic and Applied Sciences*, *1*(3-4), 151–160. https://doi.org/10.1016/j.ejbas.2014.07.002.

Engel, M., & Brückner, H. (2021). Holocene climate variability of Mesopotamia and its impact on the history of civilisation. In E. Helers, & K. Amirpur (Eds.), *Middle East and North Africa: Climate, culture and conflicts*

(pp. 77–113). Brill Publisher. https://doi.org/10.1163/9789004444973_005

Forti, L., Romano, L., Celant, A., D'Agostino, F., Di Rita, F., Jotheri, J., Magri, D., Mazzini, I., Tentori, D., & Milli, S. (2022). The paleoenvironment and depositional context of the Sumerian site of Abu Tbeirah (Nasiriyah, southern Mesopotamia, Iraq). *Quaternary Research*, 1–19. https://doi.org/10.1017/qua.2022.22

Fouad, S. F. (2010). Tectonic and structural evolution of the Mesopotamia foredeep. *Iraqi Bulletin of Geology and Mining*, *6*(2), 41–53.

Giosan, L., & Bhattacharya, J. P. (2005). New directions in deltaic studies. In L. Giosan, & J. P. Bhattacharya (Eds.), *River deltas-concepts, models, and examples* (pp. 3–10). SEPM (Society for Sedimentary Geology). https://doi.org/10.2110/pec.05.83.

Gürbüz, A., & Gürbüzb, E. (2022). Remote sensing approaches for mapping quaternary deposits: A synthesis. *Physics and Chemistry of the Earth, Parts A/B/C*, *126*, 103128. https://doi.org/10.1016/j.pce.2022.103128

Heyvaert, V. M. A., Walstra, J., Verkinderen, P., Weerts, H., & Ooghe, B. (2012). The role of human interference on the channel shifting of the Karkheh River in the lower Khuzestan plain (Mesopotamia, SW Iran). *Quaternary International*, *251*, 52–63. https://doi.org/10.1016/j.quaint.2011.07.018

Heyvaert, V. M. A., & Walstra, J. (2016). The role of long-term human impact on avulsion and fan development. *Earth Surface Processes and Landforms*, *41*(14), 2137–2152. https://doi.org/10.1002/esp.4011

Hoitink, A. J. F., Wang, Z. B., Vermeulen, B., Huismans, Y., & Kästner, K. (2017). Tidal controls on river delta morphology. *Nature Geoscience*, *10*(9), 637–645. https://doi.org/10.1038/ngeo3000

Hritz, C., & Wilkinson, T. J. (2006). Using shuttle radar topography to map ancient water channels in Mesopotamia. *Antiquity*, *80*(308), 415–424. https://doi.org/10.1017/S0003598X00093728

Iacobucci, G. (2021). *Remote sensing applications for the assessment of the geomorphic response of fluvial systems to the Holocene climate changes* [Ph.D. thesis]. Earth Sciences Department, Sapienza University of Rome, Italy. (Discussed on 15 March 2021).

Iacobucci, G., Troiani, F., Milli, S., Mazzanti, P., Piacentini, D., Zocchi, M., & Nadali, D. (2020). Combining satellite multispectral imagery and topographic data for the detection and mapping of fluvial avulsion processes in lowland areas. *Remote Sensing*, *12*(14), 2243. https://doi.org/10.3390/rs12142243

Jotheri, J. (2016). *Holocene avulsion history of the Euphrates and Tigris rivers in the Mesopotamian Floodplain*. Durham theses, Durham University. Available at Durham E-Theses Online: http://etheses.dur.ac.uk/11752/

Jotheri, J. (2018). Recognition criteria for canals and rivers in the Mesopotamian floodplain. In Y. Zhuang, & M. Altaweel (Eds.), *Water societies and technologies from the past and present* (pp. 111–126). UCL Press. ISBN 978-1-911576-69-3.

Jotheri, J., & Allen, M. (2020). Recognition of ancient channels and archaeological sites in the Mesopotamian floodplain using satellite imagery and digital topography. In *New agendas in remote sensing and landscape archaeology in the near east: Studies in honour of Tony J. Wilkinson* (pp. 283–305). Archaeopress. https://dro.dur.ac.uk/31876/

Jotheri, J., Allen, M. B., & Wilkinson, T. J. (2016). Holocene avulsions of the Euphrates river in the Najaf area of western Mesopotamia: Impacts on human settlement patterns. *Geoarchaeology*, *31*(3), 175–193. https://doi.org/10.1002/gea.21548

Jotheri, J., Altaweel, M., Tuji, A., Anma, R., Pennington, B., Rost, S., & Watanabe, C. (2018). Holocene fluvial and anthropogenic processes in the region of Uruk in southern Mesopotamia. *Quaternary International*, *483*, 57–69. https://doi.org/10.1016/j.quaint.2017.11.037

Kahle, A. B., Shumate, M. S., & Nash, D. B. (1984). Active airborne infrared laser system for identification of surface rock and minerals. *Geophysical Research Letters*, *11*(11), 1149–1152. https://doi.org/10.1029/GL011i011p01149

Karymbalis, E., Papanastassiou, D., Gaki-Papanastassiou, K., Tsanakas, K., & Maroukian, H. (2013). Geomorphological study of Cephalonia Island, Ionian Sea, Western Greece. *Journal of Maps*, *9*(1), 121–134. https://doi.org/10.1080/17445647.2012.758423

Kennett, D. J., & Kennett, J. P. (2006). Early state formation in southern Mesopotamia: Sea levels, shorelines, and climate change. *The Journal of Island and Coastal Archaeology*, *1*(1), 67–69. https://doi.org/10.1080/15564890600586283

Knight, J., Mitchell, W. A., & Rose, J. (2011). Chapter six – geomorphological field mapping. In M. J. Smith, P. Paron, & J. S. Griffiths (Eds.), *Developments in earth surface processes* (pp. 151–187). Elsevier. https://doi.org/10.1016/B978-0-444-53446-0.00006-9

Laity, J. E., & Bridges, N. T. (2013). 11.14. Abraded systems. In J. F. Shroder (Ed.), *Treatise on geomorphology* (pp. 269–286). Academic Press. https://doi.org/10.1016/B978-0-12-374739-6.00307-9

Lambeck, K. (1996). Shoreline reconstructions for the Persian gulf since the last glacial maximum. *Earth and Planetary Science Letters*, *142*(1-2), 43–57. https://doi.org/10.1016/0012-821X(96)00069-6

Landsat series. Retrieved December 15, 2021, from https://earth.esa.int/eogateway/missions/landsat

Middleton, N. J. (1986). Dust storms in the Middle East. *Journal of Arid Environments*, *10*(2), 83–96. https://doi.org/10.1016/S0140-1963(18)31249-7

Milli, S., & Forti, L. (2019). Geology and palaeoenvironment of Nasiriyah area/southern Mesopotamia. In L. Romano, & F. D'Agostino (Eds.), *Abu Tbeirah excavations I. Area 1 last phase and building A – phase 1* (pp. 19–33). Sapienza Università Editrice.

Moridnejad, A., Karimi, N., & Ariya, P. A. (2015). Newly desertified regions in Iraq and its surrounding areas: Significant novel sources of global dust particles. *Journal of Arid Environments*, *116*, 1–10. https://doi.org/10.1016/j.jaridenv.2015.01.008

Morozova, G. S. (2005). A review of Holocene avulsions of the Tigris and Euphrates rivers and possible effects on the evolution of civilizations in lower Mesopotamia. *Geoarchaeology*, *20*(4), 401–423. https://doi.org/10.1002/gea.20057

Nadali, D. (2021). Cities in the water: Waterscape and evolution of urban civilisation in southern Mesopotamia as seen from Tell Zurghul, Iraq. In L. A. Jawad (Ed.), *Southern Iraq's marshes. Their environment and conservation* (pp. 15–31). Springer International Publishing.

Nadali, D., & Polcaro, A. (2020). The Italian Archaeological Excavations at Tell Zurghul, ancient Nigin, Iraq. Final Report of the Seasons 2015-2017 (Quaderni di Vicino Oriente XVI), Sapienza Università di Roma, Roma.

Napieralski, J., Barr, I., Kamp, U., & Kervyn, M. (2013). 3.8 remote sensing and GIScience in geomorphological mapping. In J. Shroder (Ed.), *Treatise on geomorphology* (pp. 187–227). Academic Press. https://doi.org/10.1016/B978-0-12-374739-6.00050-6.

NASA Earth Observatory. (n.a.). Retrieved June 4, 2022, from https://earthobservatory.nasa.gov/images/related/39006/dust-storm-in-the-middle-east

Nehme, C., Verheyden, S., Breitenbach, S., Gillikin, D., Verheyden, A., Cheng, H., Lawrence Edwards, R., Hellstrom, J., Noble, S. R., Farrant, A. R., Sahy, D., Goovaerts, T., Salem, G., & Claeys, P. (2018). Climate dynamics during the penultimate glacial period recorded in a speleothem from Kanaan cave, Lebanon (central levant). *Quaternary Research*, *90*(1), 10–25. https://doi.org/10.1017/qua.2018.18

Olariu, C., & Bhattacharya, J. P. (2006). Terminal distributary channels and delta front architecture of river-dominated delta systems. *Journal of Sedimentary Research*, *76*(2), 212–233. https://doi.org/10.2110/jsr.2006.026

Otto, J. C., & Smith, M. J. (2013). Chapter 2: Geomorphological mapping. In S. J. Cook, L. E. Clarke, & J. M. Nielde (Eds.), *Gemorphological techniques (online edition)*. British Society for Geomorphology.

Pavlopoulos, K., Evelpidou, N., & Vassilopoulos, A. (2009). *Mapping Geomorphological Environments*, 6–46. https://doi.org/10.1007/978-3-642-01950-0

Postolenko, G. A. (1987). Large-scale geomorphological mapping. *Mapping Science and Remote Sensing*, *241*(1), 70–75. https://doi.org/10.1080/07493878.1987.10641656

Pournelle, J. R. (2003). *Marshland of cities: Deltaic landscapes and the evolution of early Mesopotamian civilization* [Unpublished Ph.D. thesis]. Department of Anthropology, University of California, San Diego.

Reddy, G. P. O. (2018). Geospatial technologies in land resources mapping, monitoring, and management: An overview. In G. Reddy, & S. Singh (Eds.), *Geospatial technologies in land resources mapping, monitoring and management. Geotechnologies and the environment* (pp. 1–18). Springer. https://doi.org/10.1007/978-3-319-78711-4

Sanlaville, P. (1989). Considérations sur l'évolution de la Basse Mésopotamie au cours des derniers millénaires. *Paléorient*, *15*(2), 5–27. https://doi.org/10.3406/paleo.1989.4506

Sanlaville, P. (2003). The deltaic complex of the lower Mesopotamian plain and its evolution through millennia. In E. Nicholson, & P. Clark (Eds.), *The Iraqi marshlands* (pp. 133–150). Politico's Publishing.

Saura, E., Garcia-Castellanos, D., Casciello, E., Parravano, V., Urrela, A., & Vergés, J. (2015). Modeling the flexural evolution of the Amiran and Mesopotamian foreland basins of NW Zagros (Iran-Iraq). *Tectonics*, *34*(3), 377–395. https://doi.org/10.1002/2014TC003660

Savelli, D., Nesci, O., Troiani, F., Dignani, A., & Teodori, S. (2012). Geomorphological map of the Montelago area (North Marche Apennines, central Italy): Constrains for two relict lakes. *Journal of Maps*, *8*(1), 113–119. https://doi.org/10.1080/17445647.2012.668771

Sissakian, V. K., Al-Ansari, N., Adamo, N., Al-Azzawi, M. K., Abdullah, M., & Laue, J. (2020). Geomorphology of the Mesopotamian plain: A critical review. *Journal of Earth Sciences and Geotechnical Engineering*, *10*(4), 1–25.

Sissakian, V. K., Al-Ansari, N., & Knutsson, S. (2013). Sand and dust storm events in Iraq. *Natural Science*, *5*(*10*), 1084–1094. https://doi.org/10.4236/ns.2013.510133

Sissakian, V. K., Shihab, A. T., Al-Ansari, N., & Knutsson, S. (2014). Al-Batin alluvial Fan, southern Iraq. *Engineering*, *6*(11), 699–711. https://doi.org/10.4236/eng.2014.611069

Steinkeller, P. (2001). New light on the hydrology and topography of southern Babylonia in the third millennium. *Zeitschrift für Assyriologie und Vorderasiatische Archäologie*, *91*(1), 22–84. https://doi.org/10.1515/zava.2001.91.1.22

Tsanakas, K., Karymbalis, E., Gaki-Papanastassiou, K., & Maroukian, H. (2019). Geomorphology of the Pieria Mtns, Northern Greece. *Journal of Maps*, *15*(2), 499–508. https://doi.org/10.1080/17445647.2019.1619630

Uuema, E., Ahi, S., Montibeller, B., Muru, M., & Kmoch, A. (2020). Vertical accuracy of freely available global digital elevation models (ASTER, AW3D30, MERIT, TanDEM-X, SRTM, and NASADEM). *Remote Sensing*, *12*(21), 3482. https://doi.org/10.3390/rs12213482

Vergari, F., Luberti, G. M., Pica, A., & Del Monte, M. (2020). Geomorphology of the historic centre of the Urbs (Rome, Italy). *Journal of Maps*, *17*(4), 6–17. https://doi.org/10.1080/17445647.2020.1761465

Verstappen, H. T. (2011). Chapter two – Old and new trends in geomorphological and landform mapping. *Developments in Earth Surface Processes*, *15*, 13–38. https://doi.org/10.1016/B978-0-444-53446-0.00002-1

Waterman, R. (2020) ArcGIS Blog. Retrieved January 24, 2022, from https://www.esri.com/arcgis-blog/products/arcgis-living-atlas/mapping/whats-new-in-world-imagery-june-2020/

Wilkinson, T. J., Rayne, L., & Jothery, J. (2015). Hydraulic landscapes in Mesopotamia: The role of human niche construction. *Water History*, *7*(4), 397–418. https://doi.org/10.1007/s12685-015-0127-9

World Imagery. Retrieved January 24, 2022, from https://www.arcgis.com/home/item.html?id=10df2279f9684e4a9f6a7f08febac2a9

Yacoub, S. Y. (2011). Geomorphology of the Mesopotamia plain. *Iraqi Bullettin of Geology and Mining*, *4*, 7–32.